ELSEVIER

Polymer 42 (2001) 9867–9876

polymer

www.elsevier.com/locate/polymer

Local chain configuration dependence of the mechanisms of chemical reactions of PVC. 8. New results from the reductive dechlorination reaction

J.M. Contreras[1], G. Martínez, J. Millán*

Instituto de Ciencia y Tecnología de Polímeros, CSIC, Juan de la Cierva 3, 28006 Madrid, Spain

Received 21 March 2001; received in revised form 10 July 2001; accepted 22 July 2001

Abstract

The reductive dechlorination of poly(vinyl chloride) (PVC) with lithium aluminium hydride, tri-*n*-butyl tin hydride and lithium triethyl borohydride as reducing agents has been performed in the solution of tetrahydrofuran. A comparative study of the microstructural evolution with conversion using the three different reducing agents was carried out. The quantitative microstructural analysis with conversion has been followed by ^{13}C NMR spectroscopy. From the evolution of the content of isotactic (**mm**), heterotactic (**mr**) and syndiotactic (**rr**) triads, and of **mmmm**, **mmmr** and **rmmr** isotactic pentads in the unmodified parts of the polymer, it is unambiguously inferred that only the central chlorine atoms of isotactic triads in **mmr** tetrads or heterotactic triads in **rmmr** pentads are reactive. This conclusion was confirmed on the basis of FTIR results. The results provide valuable information regarding the effect of tacticity and the related local conformations in the chemical reactions of PVC. © 2001 Elsevier Science Ltd. All rights reserved.

Keywords: Poly(vinyl chloride) reactions; Stereoselective reductive dechlorination; Local chain configuration

1. Introduction

Complete hydrogenation of poly(vinylchloride) (PVC) offers the possibility of elucidating defect structures in the original PVC such as chain branching. Reductive dechlorination of PVC by lithium aluminum hydride ($LiALH_4$) was first described by Cotman [1–3] and has been the object of study in numerous works [4–8]. More recently, reduction with tri-*n*-butyltin hydride (Bu_3SnH) was introduced by Starnes et al. [9] as being superior in many respects to the $LiAlH_4$ method [10–21].

The partial reduction of PVC has been used to obtain copolymers of vinyl chloride and ethylene (V–E) copolymers as an alternative route to their preparation by common copolymerization methods, which have often failed to produce copolymers with the desired composition and monomer distribution [13]. ^{13}C NMR spectroscopy was utilized to determine the compositional microstructure of the V–E copolymers with different chlorine contents. Solid-state and solution measurements [14,19] performed on these V–E copolymers have demonstrated a remarkable sensitivity of their physical properties to their compositional microstructures. However, it has not been possible to determine the stereoselective character of the reaction mechanism. In the pioneering work of Millán et al. [22], using IR analysis, it was found that the syndiotactic segments of PVC were relatively unreactive towards $LiAlH_4$ in the early stages of the reaction and they attributed the reduction to a preferential reaction of heterotactic triads. Later, Starnes et al. [9] and lately Pourahmady et al. [20] have confirmed these results.

More recently, it has been shown that nucleophilic substitution on PVC in solution proceeds by a stereospecific S_N2 mechanism in which only the last triad of isotactic sequences and the heterotactic triads adjacent to syndiotactic sequences are involved in the reaction. Thus, the reactive sites are exclusively the **mmr** tetrad and the **rrmr** pentads [23–29]. In order for these structures to react, the **mm** and **rm** triads have to take the **GTTG**$^-$ or **GTTT** conformation, respectively. **GTTG**$^-$ can exist solely at **mmr** sequences, whereas all the **mr** triads along the atactic parts can adopt **GTTT**. As the probability of **GTTG**$^-$ in PVC is very low relative to the other likely isotactic triad conformations, i.e. the unreactive **GTGT** [21–23], the conformational change ***GTGTTT*** $\Rightarrow$ ***GTTG***$^-$***TT*** at **mmr** sequences is a necessary

* Corresponding author. Tel.: +34-91-5622900; fax: +34-91-5621829.
E-mail address: jmillan@ictp.csic.es (J. Millán).
[1] Grupo de Polímeros, Departamento de Química, Facultad de Ciencias, Universidad de los Andes, Mérida 5101 A, Venezuela.

PII: S0032-3861(01)00533-X

Table 1
Reduction of PVC conditions for different agents

	PVC		Agent		AIBN (mmol)	THF (ml)	Temperature (°C)
	(g)	(mmol[a])	(g)	(mmol)			
$LiAlH_4$	4.0	64.0	2.9	17.0	–	250	40
Et_3LiBH	2.0	32.0	4.1	39.0	–	125	50
Bu_3SnH	1.6	25.0	3.5	12.0	0.32	100	60

[a] Based on monomer unit.

pre-requisite for the reaction to occur, preferably through the isotactic triads as long as they are present in the polymer [23].

It is worth noting the fact that every act of substitution not only involves the disappearance of one **mmr** or **rrmr** structure, but, owing to the inversion of the configuration of the carbon, characteristic of the S_N2 mechanism, it substantially alters the configuration and the related conformation of the adjacent triads, thereby bringing about a significant rearrangement of a definite chain segment. This consideration coupled with the aforementioned finding allowed us to propose the following stereospecific mechanisms: mechanism A applies for the reaction by the **mm** triad of **mmr** and involves the simultaneous disappearance of one isotactic triad and one heterotactic triad by exchanging for one nucleophilic group centred triad and one co-syndiotactic triad, respectively. Mechanism B is that of substitution by the **rm** triad of **rrmr** and involves the elimination of a single heterotactic triad. Finally, mechanism C relates to a well-defined fraction of **mmr** tetrads, which react by the **mr** tetrad instead of the **mm** tetrad. It involves the disappearance of one isotactic triad without the formation of one syndiotactic triad (as in mechanism A) or the disappearance of one heterotactic triad (as in mechanism B) [26].

It then appeared of great interest to investigate whether the knowledge there obtained applies to the partial reduction of PVC, taking account of the fact that the S_N2 process is the mechanism most frequently considered operating in reduction of alkyl halides. Indeed, it was important to verify whether or not the reduction reaction proceeds by the same mechanism as in the aforementioned nucleophilic substitution reactions in solution. If it were verified, it could not only provide more general conclusions concerning the effect of microstructure on the mechanism of reactions, but would make it possible to furnish by means of model polymers, some further basic support for the molecular nature of the real mechanisms involved in the physical or physico-chemical behaviour of polymer materials, as proposed in the earlier work. This is attractive because reduction, unlike nucleophilic substitution, where chlorine atoms are replaced by substituents of not much different volume and polarity, creates short polyethylenic sequences with both enhanced chain rotation motion and reduced polarity.

To do that, we have investigated herein the partial reduction of PVC using different hydride reducing agents in order to prepare V–E copolymers with differing microstructure depending on the type of the reagent, and compared them with the evolution of **mmr** and **mrr** structures, as accurately measured by ^{13}C NMR, and consequently, with the conformational changes involved in the distinct substitution process.

2. Experimental

2.1. Materials

The PVC sample studied was an additive-free commercial poly(vinyl chloride) (PVC) obtained in bulk polymerization at 70°C, where the polymerization process was stopped at a conversion of 62%. The number-average molecular weight ($M_n = 44\,000$) was determined osmometrically at 34°C in cyclohexanone at four different concentrations using a Knauer membrane osmometer. 2,2′-azodiisobutyronitrile (AIBN) from Fluka was twice recrystallized from methanol and dried under vacuum at 40°C. Tetrahydrofuran (THF) was refluxed over lithium aluminium hydride supplied by Merck to remove peroxides and distilled under nitrogen immediately before use. Cyclohexanone provided by Scharlau was purified by fractional distillation under nitrogen. $LiAlH_4$ from Merck, lithium triethylborohydride (Et_3LiBH) from Aldrich, and Bu_3SnH purchased from Aldrich were used without further purification.

2.2. Reductions of PVC using $LiAlH_4$, Et_3LiBH and Bu_3SnH

The partial reduction reactions were achieved in a three-necked Pyrex double-walled reactor equipped with an inlet tube for nitrogen, addition funnel, reflux condenser and teflon-coated magnetic stirring bar. The PVC was dissolved in THF under nitrogen atmosphere. The resulting solution was heated to the desired reaction temperature, and solutions in THF (dispersion in the case of $LiAlH_4$) of the calculated amounts of different hydride reducing agents were added dropwise (Table 1). After various reaction times, aliquot parts were added with vigorous agitation to cold methanol to precipitate the polymer. The precipitate was recovered by suction filtration and washed with methanol. All samples were purified using THF–methanol as the

solvent–precipitant system, and the product was dried in vacuum at 40°C for two days.

The degree of conversion of the reduced PVC was calculated both by ^{1}H and ^{13}C NMR spectroscopy. The mole percent of E units can be calculated from $X = 100(I_{CH2} - 2I_{CH})/(I_{CH2} + 2I_{CH})$ where I_{CH2} and I_{CH} are the integrals of methylenic (1.5–2.7 ppm) and methynic (4.3–5.0 ppm) protons, respectively. As to the ^{13}C chemical shifts, all signals upfield of 50 ppm are methylenic signals, whereas those downfield of 50 ppm represent methynic carbons [34]. Consequently, the degree of conversion can be obtained by $X = 100(I_{CH2} - I_{CH})/(I_{CH2} + I_{CH})$ where I_{CH2} and I_{CH} are the integrals of the methylenic and methynic carbons, respectively.

2.3. ^{13}C NMR spectroscopy

^{13}C NMR decoupled spectra were obtained on an XL-300 Varian instrument operating at 75.5 MHz and 90°C. The samples were examined as 10 wt% solutions using 1,4-dioxane-d_8 as solvent. The spectral width was 2500 Hz and a pulse repetition rate of 3 s and 16k data points were used. In all experiments, 15 000–20 000 scans gave a very satisfactory signal-to-noise ratio, and measuring the relative areas of different peaks by means of an electronic integrator carried out the calculations.

2.4. IR measurements

Samples were prepared as KBr pellets (3 mg of polymer/200 mg of KBr) and the IR spectra were recorded on a Nicolet 520 FTIR spectrometer equipped with a DTGS detector. 32 scans were signal-averaged at a resolution of 2 cm^{-1}. Higher resolutions (up to 0.5 cm^{-1}) gave no significant improvement of the spectra. The peak absorbances were determined from a tangent baseline.

3. Results and discussion

In the present work, partial reductions of PVC with different reducing agents have been achieved using the reaction conditions suggested by the literature [9,10,20], i.e. $LiAlH_4$ and Bu_3SnH as reducing agents used by many workers [9,10,20] and Et_3LiBH, a powerful nucleophile for S_N2 displacements [30], used recently by Pourahmady et al. [20,31]. Our experiments have been carried out under mild conditions in order to enhance the possible local configuration dependent mechanisms relating to the reduction reaction. So, we have attempted to explore a range of conversion up to about 20%. The kinetic curves for the three reducing agents utilized are shown in Fig. 1. Even though the reactivity obtained with the three reagents cannot be compared directly because of the differences in reaction conditions (e.g. reaction temperature about 20°C lower for $LiAlH_4$), Fig. 1 shows that Bu_3SnH is the most reactive reagent at the experimental conditions used, displaying a very fast rate during all the range of conversions studied. A possible explanation lies in the fact that the reaction takes place in the presence of a radical initiator via the free radical process and consequently, the rate-determining step (attack by the tributyltin radical on the alkyl halide) ought to be accelerated by electron-withdrawing substituents in the alkyl radical [32]. The other two agents seem to have two periods, one steep period followed by a slower one. This behaviour is particularly marked in the reaction with $LiAlH_4$, which exhibits an analogous kinetic curve to that found for nucleophiles when the substitution reaction is achieved at low reaction temperature [33]. Accordingly, it seems very exciting to us to investigate the possible differences in the structural selectivity in the reduction reaction depending on the type of the agent used. The change of slope in the kinetic curves of the last two agents takes place at around 8–9% conversion. Clearly, this indicates that each period is related to the reactivity of well-defined structures. However, what is important for the purpose of the present research is to realize that this change is similar to that observed in the nucleophilic substitution reaction, i.e. when the more reactive isotactic **mm** triads have disappeared and the reaction continues more slowly at the heterotactic **rm** triads. This observation is in accordance with expectation because the reaction could proceed through a stereoselective mechanism mainly with $LiAlH_4$.

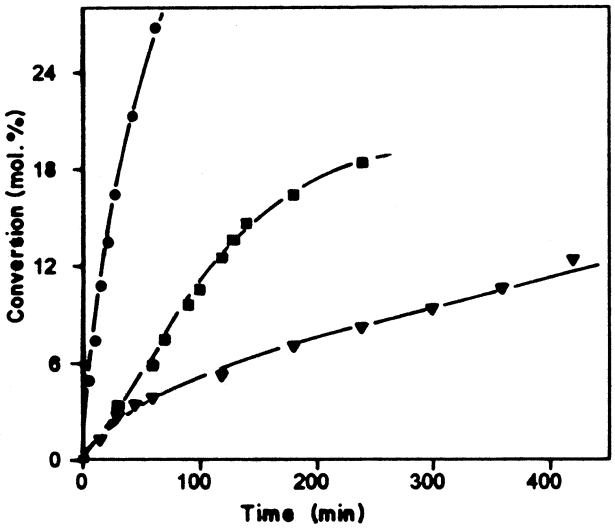

Fig. 1. Reductive dechlorination of PVC with different reagents: (▼) $LiAlH_4$; (■) Et_3LiBH; (●) Bu_3SnH (see Table 1).

Two aspects are of special interest as to the characterization of the samples studied in the present work, namely the comonomer composition and the evolution of tacticity with conversion. First of all, the concentration of comonomer units in reduced PVC (V–E copolymers) which varies with the composition, can be easily determined by ^{13}C NMR spectroscopy [34] (Fig. 2). The integration of the areas of the different resonances allows the evaluation of comonomer sequence probabilities (dyad and triads) as well as the overall comonomer composition of V–E copolymers.

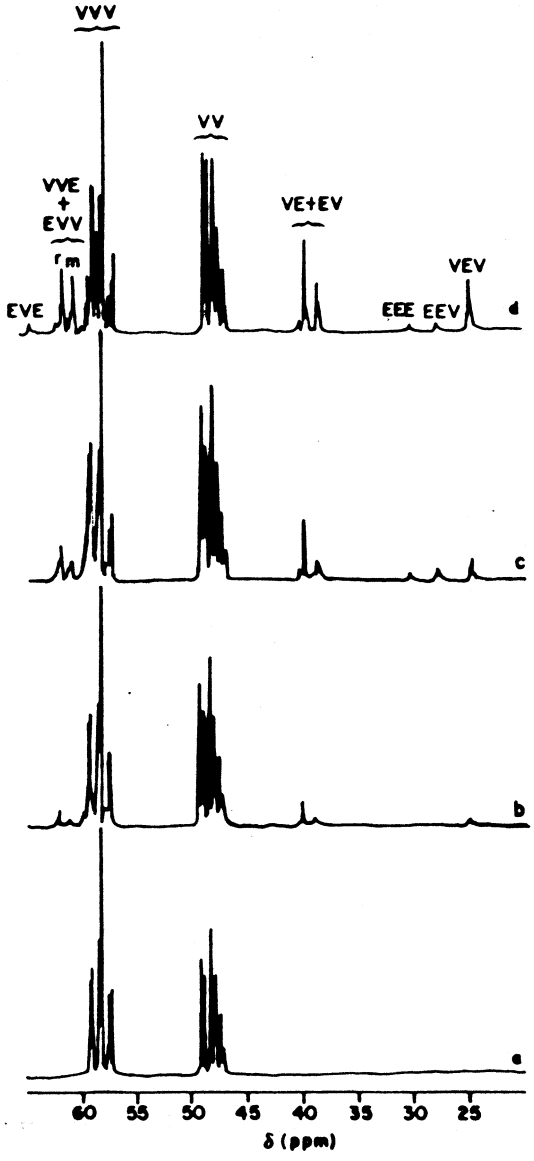

Fig. 2. ^{13}C NMR spectra of PVC reduced with Et_3LiBH at various conversions: (a) 0%; (b) 5.9%; (c) 12.5%; (d) 14.6%.

The results are collected in Tables 2–4. The most salient feature is that the EE dyad and EEE triad begin to appear at conversions around 7%, irrespective of the reducing agent used. This value corresponds approximately to the end of the first period observed in the kinetic curves (Fig. 1). This is important since it suggests clearly the existence of a specific fraction of structures in the PVC with an enhanced reactivity and, therefore, the possible existence of stereoselectivity in the reaction. Nevertheless, this result reveals nothing about the nature of the type of structures involved in this period and therefore, it is important to elucidate whether the reduction of PVC proceeds via a stereospecific mechanism, i.e. if the isotactic and heterotactic triads are the only ones to participate in the reaction as previously found for nucleophilic susbstitution [23–29].

On the other hand, the inversion of configuration of the carbon atom when undergoing an S_N2 attack was shown to produce important changes in the tacticity of the unreacted parts of the polymer [23–29]. Actually, S_N2 substitution on, e.g. the **mm** triad of **mmrm** pentad makes this pentad change into **rrrm** configuration. In contrast, in the case of reduction of PVC through an S_N2 mechanism, a methynic carbon is converted into a methylene carbon, which unlike the case of nucleophilic substitution, involves no appearance of new signals of methynic carbon, but results in the removal of the reactive triads.

With respect to the evolution of tacticity, Fig. 3 gives an overview of the ^{13}C NMR spectrum with the conversion. We focus our attention on the resonances between 57.0 and 59.7 ppm, which correspond to the methynic carbon (VVV triads). The content of unreacted iso, hetero and syndiotactic triad at any degree of conversion can be determined from the set of signals centred around 57.5, 58.5 and 59.2 ppm, respectively, provided that they be separated enough for their areas to be measured accurately. Furthermore, such a resolution makes it possible to follow, at least to some extent, the changes in **rmmmrx** and **mmmmrx** ($x =$ **m** or **r**) isotactic heptad content as the degree of substitution increases [23]. It is worth noting that, as mentioned

Table 2
Dyad and triad probabilities (V and E units) of PVC reduced with $LiAlH_4$

Conversion (mol% E)	P_{VV}	$P_{VE} + P_{EV}$	P_{EE}	P_{VVV}	$P_{VVE} + P_{EVV}$	P_{VEV}	$P_{VEE} + P_{EEV}$	P_{EVE}	P_{EEE}
0	100	–	–	100	–	–	–	–	–
1.3	97.6	2.4	–	95.1	2.6	2.3	–	–	–
3.4	95.9	4.1	–	92.4	3.8	3.8	–	–	–
3.9	92.8	7.2	–	89.7	4.9	5.4	–	–	–
5.2	89.5	10.5	–	85.8	8.5	5.7	–	–	–
7.1	86.5	13.0	0.5	82.1	11.1	6.8	–	–	–
9.4	83.5	15.4	1.1	75.9	13.6	7.8	1.3	0.7	0.7
10.6	78.4	19.7	1.9	69.0	17.4	9.7	1.4	1.6	0.9
12.3	74.3	21.9	3.6	62.1	19.3	11.2	1.7	4.5	1.2

Table 3
Dyad and triad probabilities (V and E units) of PVC reduced with Et_3LiBH

Conversion (mol% E)	P_{VV}	$P_{VE} + P_{EV}$	P_{EE}	P_{VVV}	$P_{VVE} + P_{EVV}$	P_{VEV}	$P_{VEE} + P_{EEV}$	P_{EVE}	P_{EEE}
0	100	–	–	100	–	–	–	–	–
3.4	95.4	4.6	–	95.3	2.6	2.1	–	–	–
5.9	93.7	6.3	–	93.0	5.7	1.3	–	–	–
7.5	90.0	8.0	2.0	85.2	9.8	3.7	1.0	–	0.9
9.6	89.8	7.4	2.8	84.4	9.4	4.0	0.8	–	0.6
10.5	85.0	8.2	6.8	78.7	12.2	5.1	1.9	–	2.1
12.5	80.2	13.8	6.0	78.1	12.8	4.9	1.6	–	2.6
13.5	78.0	14.8	7.2	76.0	13.9	5.3	2.0	–	2.8

before, the reduction of PVC, unlike nucleophilic substitution, does not bring about the appearance of new bands close to the triads of unmodified PVC. Consequently, the total content of tactic triads will refer, irrespective of degree of conversion, to the value of 100. Nevertheless, the reduction reaction is expected to involve necessarily important changes in the tacticity because of the new order along the polymer chain. Whether, and to what extent, this change disturbs the overall balance of the isotactic and syndiotactic configurations will depend on the specific reactivity they have in S_N2 mechanism.

In the reduction of PVC contrary to what happens in nucleophilic substitution reaction, each act of substitution of chlorine atom does not carry out the apparition of cotacticity because the reduction of the CHCl results in a sequence of three methylene groups where there is no tacticity. Consequently, the following changes are expected to occur for each of the reaction mechanisms proposed in previous works [26–29,35]:

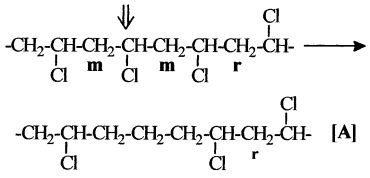

this substitution (mechanism A) involves the simultaneous disappearance of one isotactic triad and one heterotatic triad;

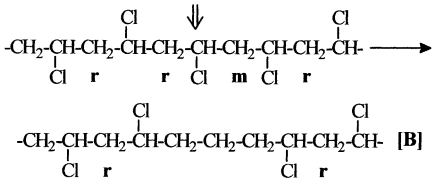

where (mechanism B) one syndiotactic triad and two heterotactic triads disappears;

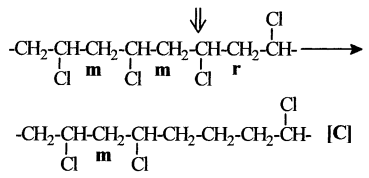

this mechanism (mechanism C) involves the elimination of one isotactic triad and one heterotactic triad.

As can be seen from Fig. 3, these changes agree with experience. Comparing the spectra in Fig. 3, it is apparent that the increase in syndiotactic triad content is related to the disappearance of the isotactic triad content. A quantitative indication of this behaviour is the evolution of the ratio of **r** to **m** dyads with conversion. This ratio is 1.27 for the unmodified polymer, a Bernoullian sample of $P_m = 0.440$. The removal of 12.5% of the chlorine atoms (sample c, Fig. 3) causes the **r/m** ratio to increase and this effect appears to depend on the reducing agent: Bu_3SnH (1.36); $LiAlH_4$ (1.54) and Et_3LiBH (1.66). Clearly, Cl atoms in **m** dyads are, as a whole, more reactive than those in **r** dyads, and this discrimination depends on the nature of the reducing agent. From these results, it follows that the reduction

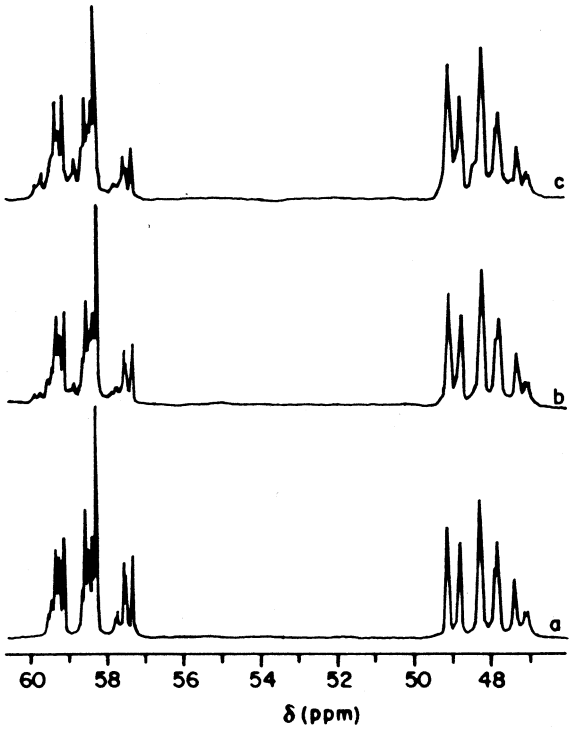

Fig. 3. ^{13}C NMR spectra (methynic and methylenic) of PVC reduced with Et_3LiBH at various conversions: (a) 0%; (b) 5.9%; (c) 12.5%.

Table 4
Dyad and triad probabilities (V and E units) of PVC reduced with Bu_3SnH

Conversion (mol% E)	P_{VV}	$P_{VE} + P_{EV}$	P_{EE}	P_{VVV}	$P_{VVE} + P_{EVV}$	P_{VEV}	$P_{VEE} + P_{EEV}$	P_{EVE}	P_{EEE}
0	100	–	–	100	–	–	–	–	–
2.0	97.7	2.3	–	95.6	0.7	3.7	–	–	–
2.5	96.5	3.5	–	95.1	1.3	3.5	–	–	–
5.1	94.7	5.3	–	92.0	2.5	3.6	–	–	–
7.4	92.1	7.8	–	87.5	4.8	3.9	–	–	–
10.9	87.3	11.1	1.6	82.6	10.1	6.2	0.6	–	0.5
13.5	82.8	11.4	5.8	74.9	11.3	10.1	1.6	–	2.1

with $LiAlH_4$ and Et_3LiBH is more stereoselective than with Bu_3SnH. This point is better illustrated by Fig. 4, which refers to the evolution of the content of each triad with the degree of conversion. As can be observed, the isotactic triad content decreases with increasing degrees of conversion, this effect being much more pronounced for the reactions with $LiAlH_4$ and Et_3LiBH. The heterotactic triad content remains practically unchanged except for $LiAlH_4$ and Bu_3SnH where it decreases slowly from about 6% conversion. Correspondingly, the syndiotactic triad content increases with degree of conversion. As can be seen, two well-differentiated steps are apparent. The slope in the second step decreases as the heterotactic triad content decreases when the conversion exceeds 6% for $LiAlH_4$ and Et_3LiBH reagents. The results in Fig. 4 show again that the reaction with $LiAlH_4$ and Et_3LiBH is more stereoselective than that with Bu_3SnH. The results shown so far seem to prove the high reactivity of **mmr** tetrads in the reduction reaction.

The percent of disappearance of **mm** triads with degree of reduction is plotted in Fig. 5. Since in the case of Bu_3SnH, a radical mechanism of reduction is known to compete with the S_N2 based mechanism cited above, special attention would be paid to $LiAlH_4$ and Et_3LiBH reactants. As indicated by the overall loss of isotactic triads, mechanism A predominates for both reactants. As can be seen, there appear to be two stages of reaction: before and after 6% conversion. The magnitude of the slope changes when passing from one period to the other. During the former, $LiAlH_4$ presents a higher slope, which corresponds to a higher contribution of mechanism A compared to mechanism B. However, a slight change in the slope happens at around 5%, which indicates, following the results obtained in the nucleophilic substitution reaction, an increase in the proportion of mechanism B, i.e. of the reaction through **rrmr** structures. Besides, the implication of the reaction via **rrmr** during the second period, relative to **mmr**, would have to result in the decrease of the heterotactic triad content, which is in accordance with experience (Fig. 4).

Comparing the slopes for $LiAlH_4$ and Et_3LiBH, it is clear that the ratio between mechanisms A and B is reduced or reverted for $LiAlH_4$ and Et_3LiBH, respectively, at conversions ranging from 5 to 6%, probably because in the case of $LiAlH_4$, the **mmr** linked with long isotactic sequences

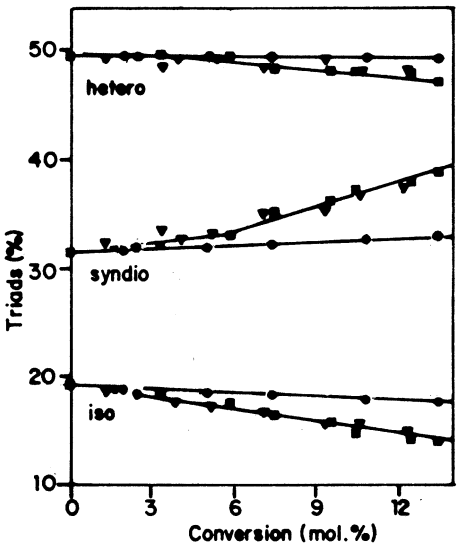

Fig. 4. Evolution of the content of the tactic triads with the reduction of PVC with different reagents: (▼) $LiAlH_4$; (■) Et_3LiBH; (●) Bu_3SnH.

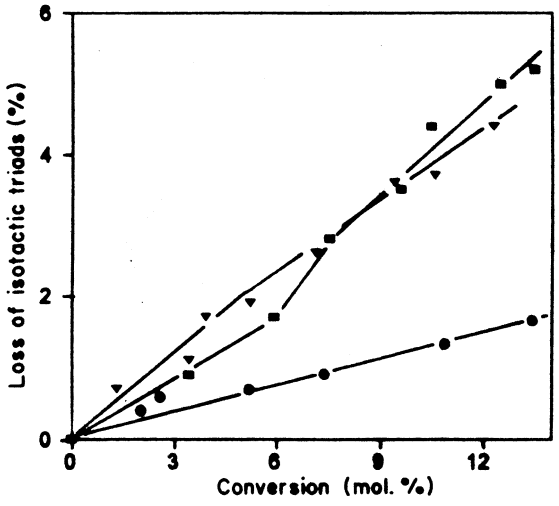

Fig. 5. Evolution of loss of isotactic triads with the reduction reaction: (▼) $LiAlH_4$; (■) Et_3LiBH; (●) Bu_3SnH.

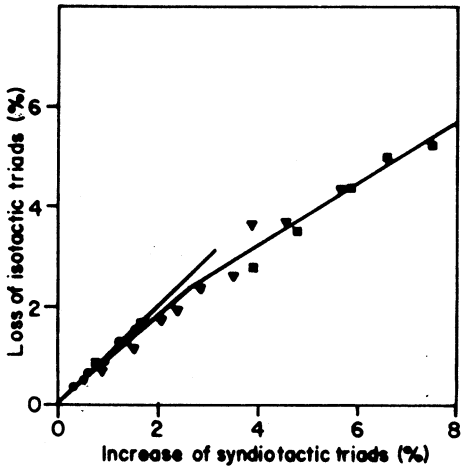

Fig. 6. Evolution of loss isotactic triad versus increase syndiotactic triads: (▼) $LiALH_4$; (■) Et_3LiBH; (●) Bu_3SnH.

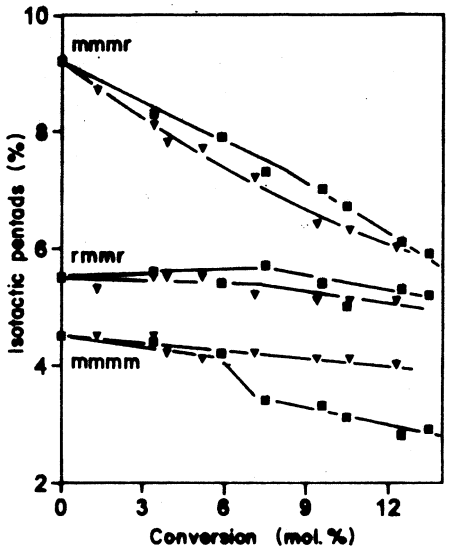

Fig. 8. Evolution of isotactic pentads with the reduction of PVC with (▼) $LiALH_4$ and (■) Et_3LiBH.

become scarce and in the case of Et_3LiBH, the reactivity of **mmr** in short isotactic sequences irrespective of mechanism A or C and the reactivity of **rrmr** (mechanism B) are not so much different from or higher than that of **mmr** terminal of long sequences.

It is then worthwhile to note that the effectiveness of mechanism B, i.e. the attack through **mr**, is accentuated from around 6% which is just the level of conversion where the relative implication of the reduction reaction via **mmr** or **rrmr** is altered. As a first approximation, this difference is similar to that found in nucleophilic substitution reaction.

The occurrence of the attack through **mr** in **mmr** (mechanism C) cannot be discriminated experimentally from the attack through **mm** in the same **mmr** tetrad (mechanism A) because they both involve the same change, i.e. the loss of one isotactic and one heterotactic triad.

Finally, Fig. 6 depicts the isotactic triad loss versus the syndiotactic triad increase. From such a plot, it is apparent that there are two well-defined steps, the slope of which changes around 6% in accordance with the discrimination between both **mmr** and **rrmr** species. This is consistent with the evolution of the ratio between mechanisms A and B with conversion, as discussed above, and lends support for the correlation between mechanisms A and B and the isotactic dyad of **mmr** and **rrmr**, respectively, thereby accounting for the stereospecific nature of the reduction reaction.

However, the question arises as to whether the reactivity of **mmr** depends markedly on the length of the isotactic sequence on the left side, as happens in substitution reactions-. The answer to this question follows straightforwardly from the result of Figs. 7–9. Fig. 7 exhibits the changes in the pentad and heptad bands with degree of reduction. An evaluation of these changes is shown in Figs. 8 and 9. Fig. 8 depicts the loss of each of the isotactic pentads, as determined from the corresponding areas in the ^{13}C NMR spectrum versus conversion. It is quite apparent that the reactivity of **mmmr** is markedly higher than that of the other pentads irrespective of the reagent used, though this reactivity is more evident with $LiAlH_4$ which indicates a higher stereoselectivity of this reagent against Et_3LiBH. On the other hand, it is noteworthy that the evolution of the **mmmr** isotactic pentad with conversion is higher than that obtained on nucleophilic substitution reaction [26–29,35] which indicates the higher implication of mechanism A as pointed out before. Fig. 9 shows the percent loss of each of the isotactic heptads with conversion. It may be

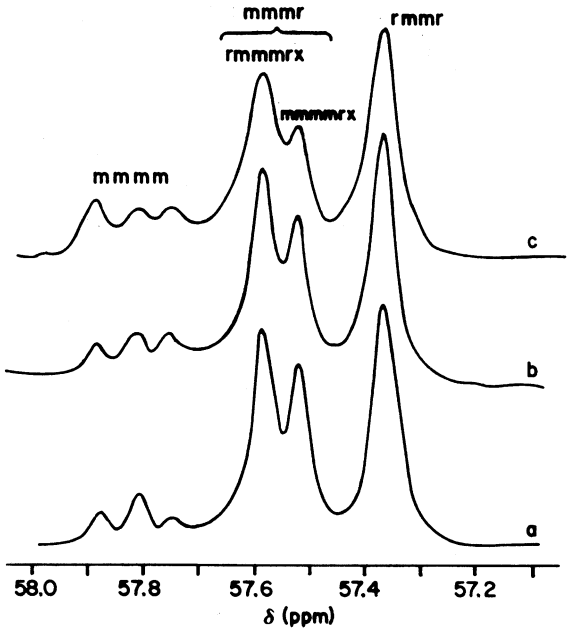

Fig. 7. Evolution of ^{13}C NMR spectra (isotactic pentads) with the reduction reaction ($LiAlH_4$): (a) 0%; (b) 5.9%; (c) 12.5%.

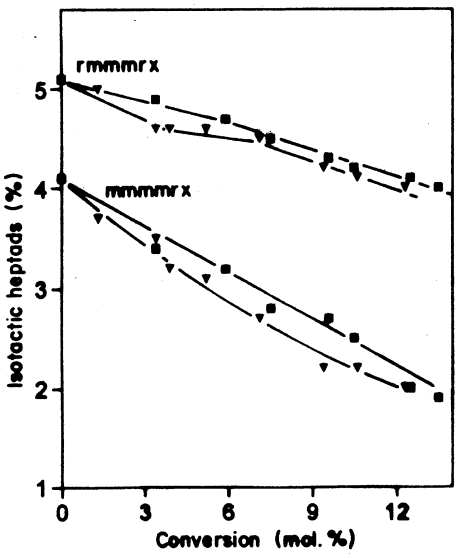

Fig. 9. Evolution of isotactic heptads in **mmmr** centred pentads with the reduction of PVC with (▼) $LiAlH_4$ and (■) Et_3LiBH.

appreciated that the higher slope corresponds to the loss of **mmmmrx** heptad; thus, the reactivity of **mmr** proves to be much more accentuated as the length of the associated isotactic sequence increases which strongly confirms the stereoselective nature of the reduction of PVC.

As shown in earlier work, the nucleophilic substitution reaction cause the involved local configurations and the respective local conformations, to be altered so that the conformationally sensitive C–Cl vibrations bands of the FTIR spectrum of PVC should be expected to change with substitution. In fact, the experimental changes in the bands, in particular, those at 600–700 cm^{-1} region prior to and after substitution, were found to be in close agreement with theoretical expectations which proved to support strongly the local configurational nature of the mechanisms of analogous reactions of PVC [28,29,35,36].

With the aim of checking whether the above-proved

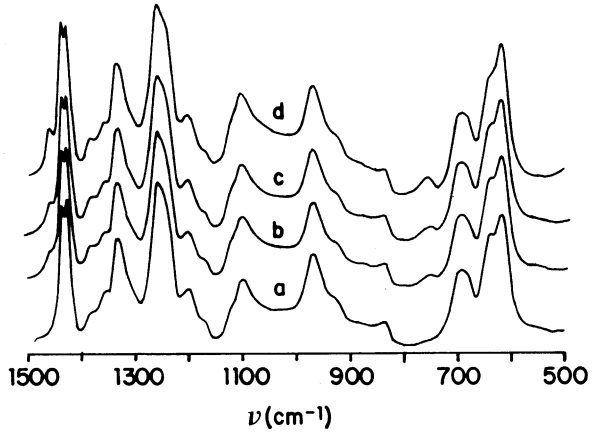

Fig. 10. Evolution of infrared spectra with the reduction reaction ($LiALH_4$): (a) 0%; (b) 3.9%; (c) 5.2%; (d) 9.4%.

stereoselectivity of reduction of PVC agrees with the FTIR results found in nucleophilic substitution reaction, this technique was also applied to the same samples measured by ^{13}C NMR. Fig. 10 shows the 500–1500 cm^{-1} region of the FTIR spectrum of the virgin PVC sample and the same sample after different degrees of reduction with $LiAlH_4$. A glance at the spectra shows that some new bands arise at 1434 cm^{-1} and 760 cm^{-1} as the chlorine atom are removed from PVC by exchanging for hydrogen atoms. The former band has been assigned to C–H bending modes in polyethylene [37] and is overlapping the bands at 1428 and 1434 cm^{-1} which are due to δ vibrations of CH_2 in PVC. The band at 760 cm^{-1} has been assigned to the rocking motion of central CH_2 (3 or 5) in –VEV– triad or –VEEV– tetrad sequences [38]. However, the most significant bands for purposes of polymer microstructure are known to be the bands between 600 and 700 cm^{-1} (ν, C–Cl vibrations).

The assignment of the ν(C–Cl) bands of PVC has been well documented [39]. As a whole, the bands at 693 and 685 cm^{-1}, usually overlapped, are due to S_{HC} absorption modes, whereas the bands at 615 and 637 cm^{-1} obey S_{HH} absorption modes of C–Cl bond (the suffix stands for the *trans* substituents on both C–C bonds adjacent to the C–Cl bond). It then follows that these bands are very sensitive to the local chain conformations and, owing to the microstructure dependence of the latter, to the local microstructure of the polymer.

Besides, each of these frequencies has been proved, both experimentally and theoretically, to depend on the local environment in which they find themselves [40]. In this connection, the S_{HH} C–Cl bond in all-*trans* syndiotactic sequences are known to exhibit two bands at around 640 and 602 cm^{-1} (the actual frequency varies somewhat with the length of the syndiotactic sequences) [40]. The bond, $(S_{HH})_a$, is necessarily flanked by two similar S_{HH} C–Cl bonds ($S_{HH}{\cdot}(S_{HH})_a{\cdot}S_{HH}$ C–Cl group sequence in TTTT syndiotactic triad conformation), which enables two well-differentiated stretching modes to originate from the intramolecular interaction with the adjacent C–Cl groups. This accounts for the observed pair of bands [40].

Departures from the extended TTTT syndiotactic local conformation, whether they arise from rotations about C–C bonds or, most usually, from departures from stereoregularity, result necessarily in the presence of S_{HH} C–Cl bonds with one or two S_{CH} adjacent C–Cl bonds. This is what happens for the central chlorine of the

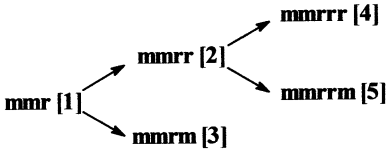

Scheme 1.

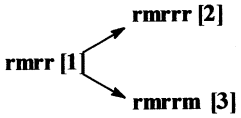

Scheme 2.

GTTT heterotactic triad conformation, $(S_{HH})_b$, and of the **GTTG**$^-$ isotactic triad conformation, $(S_{HH})_c$, respectively. The corresponding C–Cl bond sequences are $S_{CH}{\cdot}(S_{HH})_b{\cdot}S_{HH}$ and $S_{CH}{\cdot}(S_{HH})_c{\cdot}S_{HC}$.

We have designed by $(S_{HH})_a$, $(S_{HH})_b$, and $(S_{HH})_c$ the foregoing types of C–Cl bond and the respective stretching frequences. As extensively argued in the literature [40,41], $(S_{HH})_b$ and $(S_{HH})_c$ are not perturbed by intramolecular interactions with the adjacent C–Cl group certainly because the latter, unlike the ones adjacent to $(S_{HH})_a$, are not coplanar; thus, a single frequency is expected in each case. Many scientists have agreed to attribute the bands at 612 and 622 cm^{-1} (usually overlapped by the former) to $(S_{HH})_b$ and $(S_{HH})_c$ modes, respectively [41].

Consequently, we are interested in estimating theoretically the changes in either the sequential order or, especially, the number of $(S_{HH})_a$, $(S_{HH})_b$ and S_{HC} modes derived from reduction. These changes enable the evolution of the band at 615, 637 and 690 cm^{-1}, respectively, to be predicted theoretically [36]. To accomplish this task, we select those sequences derived from the reactive structures **mmr** and **rmmr**, which contain all the potentially changing C–Cl bonds with reduction by each of the reactive structures (Schemes 1 and 2).

The corresponding changes in absorption mode coupled with the changes in the contents of the distinct types of C–Cl bond and to the expected evolution of the corresponding IR bands are compiled by Tables 5 and 6.

The next step is to analyse the experimental results obtained in Fig. 10 in relation with the evolution of the 615, 637 and 685 cm^{-1} bands for the changes in local microstructure derived from reduction reaction. Clearly, no change in the positions of 615 and 637 cm^{-1} bands is observed. Instead, by inspection, the following changes may be tentatively drawn: the intensity of the band at

Table 5
Implications of reduction reaction by **mmr**-based structures (Scheme 1)

Configuration	C–Cl absorption modes		FTIR C–Cl bands (cm^{-1})
	Mechanism A	Mechanism C	
1–5	-2 [S_{HC}]		↓690
	$+1$ [$(S_{HH})_b$]		↑615
3		-1 [S_{HC}]	↓690
4		-1 [S_{HC}]	↓690
		$+1$ [$(S_{HH})_b$]	↑615
		-1 [$(S_{HH})_a$]	↓637
5		-1 [S_{HC}]	↓690

Table 6
Implications of reduction reaction by **mmr**-based structures (Scheme 2) (only mechanism B)

Configuration	C–Cl Absorption modes	FTIR C–Cl bands (cm^{-1})
–rmrrr–	-1 [$(S_{HH})_a$]	↓637
	$+1$[$(S_{HH})_b$]	↑615
–rmrrm–	-1 [$(S_{HH})_b$]	↓615

615 cm^{-1} increases compared to that of 637 cm^{-1}; on the other hand, it becomes narrower and more symmetrical. The band at 637 cm^{-1} seems to decrease in a parallel, although slower, way to the increase of the 615 cm^{-1} bands. It is notable that the decrease in the 637 cm^{-1} bands occurs at conversions between 5 and 9% (spectra **c** and **d**, respectively).

The changes in the intensity of 615 and 637 cm^{-1} bands are illustrated in a quantitative way through the evolution of the absorbance ratio A_{615} cm^{-1}/A_{637} cm^{-1} with conversion (Fig. 11). As can be seen, this ratio increases throughout the range of reaction studied, but two well-differentiated stages are apparent. The first stage clearly corresponds to the occurrence of mechanism A through the **mm** triad of **mmr** tetrad which gives rise to the appearance of one new $(S_{HH})_b$ (increase of 615 cm^{-1}). The increase of the slope during the second stage is in agreement with the implication of mechanisms B and C which brings about the disappearance of one $(S_{HH})_a$ mode (decrease of 637 cm^{-1}) and the stabilization of 615 cm^{-1} band as a consequence of the depletion of the **mmr** tetrad of high reactivity associated with long isotactic sequences. On the other hand, in the case of HLi in both stages, the increase of the A_{615} cm^{-1}/A_{637} cm^{-1} ratio is higher than with SH, which as found previously, is a consequence of the higher stereospecific nature of the former favouring the mechanism A whenever the reactive structures **mmr** are present. The results of Fig. 12, which depicts the evolution of A_{615} cm^{-1}/A_{690} cm^{-1} ratio with conversion, confirm those found in Fig. 11. In fact, the first stage of the reaction is a contribution of each reagent to mechanism A and the

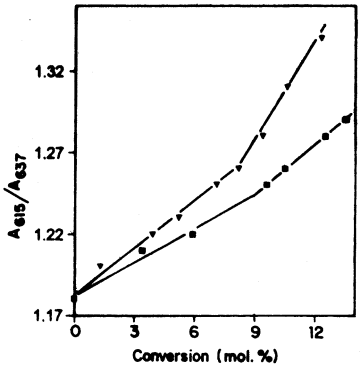

Fig. 11. Evolution of the IR absorbance ratio A_{615} cm^{-1}/A_{637} cm^{-1} with the reduction of PVC with (▼) $LiAlH_4$ and (■) Et_3LiBH.

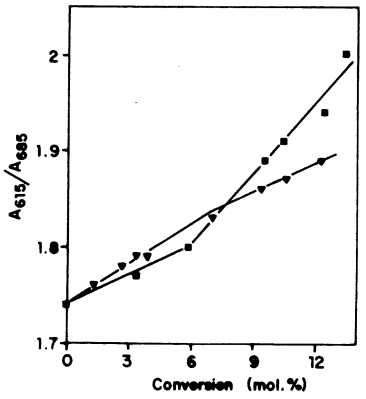

Fig. 12. Evolution of the IR absorbance ratio A_{615} cm^{-1}/A_{685} cm^{-1} with the reduction of PVC with (▼) $LiALH_4$ and (■) Et_3LiBH.

increase of the slope around 8% indicates the occurrence of mechanism C going rise the disappearance of S_{HC} absorption mode (decrease of 690 cm^{-1}).

It thus follows that the experimental behaviour of the ν C–Cl bands is in close agreement with the theoretical expectations, which enables the mechanisms A–C to be correlated with the local environment in which each of the reactive structures, **mmr** or **rmmr**, finds itself.

Basically, the results presented herein demonstrate the highly stereospecific nature of the reductive reaction of PVC mainly when the reaction is carried out with $LiAlH_4$ which proceeds by the same mechanisms found in nucleophilic substitution reaction, so providing a conclusive approach to the local configurational nature of the mechanisms of chemical reactions of polymers.

Acknowledgements

We are grateful to the Dirección General de Investigación Científica y Técnica (DGICYT) for the financial support (PB 93-1250).

References

[1] Cotman Jr JD, Ann NY. Acad Sci 1953;57:417.
[2] Cotman Jr JD. Am Chem Soc 1955;77:2790.
[3] Cotman Jr JD. US Patent, 2 716 642, 1955.
[4] Abbas KB, Bovey FA, Schilling FC. Makromol Chem Suppl 1975;1:227.
[5] Bovey FA, Abbas KB, Schilling FC, Starnes Jr WH. Macromolecules 1975;8:437.
[6] Starnes Jr WH, Hartless RL, Schilling FC, Bovey FA. Polym Prepr ACS 1977;18:499.
[7] Starnes Jr WH, Schilling FC, Piltz IM, Hartless RL, Bovey FA. Polym Prepr ACS 1978;19:579.
[8] Tonelli AE, Schilling FC. Macromolecules 1981;14:74.
[9] Starnes Jr WH, Schilling FC, Abbas KB, Piltz IM, Hartless RL, Bovey FA. Macromolecules 1979;12:13.
[10] Hjertberg T, Wendel A. Polymer 1982;23:1641.
[11] Starnes Jr WH, Schilling FC, Piltz IM, Casi RE, Freed DJ, Hartless RL, Bovey FA. Macromolecules 1983;16:790.
[12] Starnes Jr WH, Villacorta GM, Schilling FC, Piltz IM, Park GS, Saremi AH. Macromolecules 1985;18:1780.
[13] Schilling FC, Tonelli AE, Valenciano M. Macromolecules 1985;18:356.
[14] Bowmer TN, Tonelli AE. Polymer 1985;26:1195.
[15] Braun D, Mao W, Böhringer B, Garbella RW. Angew Makromol Chem 1986;141:113.
[16] Jameison FA, Schilling FC, Tonelli AE. Macromolecules 1986; 19:2168.
[17] Jameison FA, Schilling FC. ACS Symp Ser 1989;364:356.
[18] Gómez MA, Tonelli AE, Lovinger AJ, Schilling FC, Cozine MH, Davis DD. Macromolecules 1989;22:4441.
[19] Tonelli AE, Schilling FC, Bowmer TN, Valenciano M. Polym Prepr ACS 1983;24:211.
[20] Pourahmady N, Bak PI, Kinsey RA. JMS Pure Appl Chem 1992; A29:959.
[21] Scherrenberg RL, Reynaers H, Gondard C, Verluyten JP. Macromolecules 1993;26:4118.
[22] Millán J, Arranz F, Pinzón E. Rev Plást Mod 1974;27:361.
[23] Millán J, Martínez G, Jimeno ML. Eur Polym J 1991;27:483.
[24] Martínez G, Guarrotxena N, Gómez-Elvira JM, Millán J. Polym Bull 1992;28:427.
[25] Guarrotxena N, Martínez G, Gómez-Elvira JM, Millán J. Macromol Rapid Commun 1994;15:189.
[26] Guarrotxena N, Martínez G, Millán J. J Polym Sci Polym Chem 1996;34:2387.
[27] Guarrotxena N, Martínez G, Millán J. Polymer 1999;40:629.
[28] Martínez G, García C, Guarrotxena N, Millán J. Polymer 1999;40:1507.
[29] Guarrotxena N, Martínez G, Millán J. Acta Polym 1999;50:180.
[30] Brown HC, Krishnamurthy S. J Am Chem Soc 1973;95:1669.
[31] Pourahmady N, Bak PI. JMS Pure Appl Chem 1994;A31:185.
[32] Fort Jr RC, Hiti J. J Org Chem 1977;42:3968.
[33] Martínez G, Mijangos C, Millán J. Polym Bull 1990;23:233.
[34] Tonelli AE. NMR spectroscopy and polymer microstructure: the conformational connection. New York: VCH, 1989. p. 139.
[35] Martínez G, Millán J. Macromol Chem Phys 2000;201:1709.
[36] Guarrotxena N, Martínez G, Millán J. J Polym Sci 1996;34:2563.
[37] Bowmer TN, Tonelli AE. J Polym Sci Polym Phys 1986;24:1631.
[38] Bucci G, Simonazzi T. J Polym Sci, Part C 1964;7:203.
[39] Krimm S, Folt VL, Shipman JJ, Berens AR. J Polym Sci 1963;A1:2621.
[40] Shimanouchi T, Tasumi M, Abe Y. Makromol Chem 1965;86:43.
[41] Bower DI, Jackson RS. J Polym Sci Polym Phys 1990;28:1589.